Comparison of MRI T2 Mapping and T2 Multi-Echo 3D Water Excitation in Assessing Cartilage Injury of Ankle Joint

Ann. Ital. Chir., 2026 97, 4: 741–752
https://doi.org/10.62713/aic.4197

Si Chen[1,†], Jiacheng Zang[2,†], Lin Guo[1], Hui Zhao[1], Xin Wan[3]

[1]Radiology Department, Tianjin Hospital, 300211 Tianjin, China
[2]Department of Hip Traumatology, Tianjin Hospital, 300211 Tianjin, China
[3]Ultrasonic Department, Tianjin Hospital, 300211 Tianjin, China

AIM: The ankle joint is vulnerable to injuries. However, utilizing conventional magnetic resonance imaging (MRI) to detect early compositional changes of cartilage injury in the ankle joint poses significant challenges, and the diagnostic value of T2 mapping and T2 multi-echo 3D water excitation (T2-me3d-we) versus conventional MRI remains unclear. To explore the clinical value of T2 mapping and T2-me3d-we quantitative parameters in MRI in the diagnosis of cartilage injury of the ankle joint based on the receiver operating characteristic (ROC) curve.

METHODS: Clinical data of 182 patients with suspected cartilage injury of the ankle joint who underwent MRI examination in our hospital from November 2019 to November 2021 were retrospectively analyzed. T2 mapping and T2-me3d-we quantitative parameters were obtained from MRI examination performed on all included patients. T2 values, apparent diffusion coefficient (ADC) and fractional anisotropy (FA) were measured as key parameters. ROC curve analysis, paired *t*-test, and intraclass correlation coefficient (ICC) were used for comparative analysis.

RESULTS: T2 mapping demonstrated superior efficacy, as evidenced by a higher area under the curve (AUC) (0.879 vs. 0.868) and a higher Youden index (0.608 vs. 0.607) in the ROC analysis. The combination of T2 mapping–derived T2 values and diffusion tensor imaging ADC metrics using an integrated model achieved an AUC of 0.942 (95% confidence interval [CI]: 0.897–0.987). This result indicates that the model performed better than the performance of each individual parameter when used on its own. The diagnostic coincidence rate of T2 mapping was 97.80%, higher than the T2-me3d-we rate of 93.41% ($p < 0.05$). Compared with the normal group (NG), the injury group (IG) exhibited higher T2 values ($p < 0.001$) and ADC values, but lower FA values ($p < 0.001$). The ROC curve showed that the quantitative parameters of T2 mapping and T2-me3d-we demonstrated good diagnostic efficacy for cartilage injury of the ankle joint.

CONCLUSIONS: T2 mapping demonstrated superior quantitative diagnostic performance compared to T2-me3d-we for detecting ankle chondral lesions and may therefore serve as a promising first-line imaging biomarker for routine clinical evaluation. Combined image assessment further enhanced discriminatory power, offering incremental value for surgical decision-making.

Keywords: cartilage injury of ankle joint; magnetic resonance imaging; T2 mapping; MRI water excitation; ROC curve

Introduction

Ankle joint injury accounts for approximately 15% of all musculoskeletal injuries, with over 40% of cases involving articular cartilage damage, particularly in young and middle-aged athletes [1]. Talar cartilage lesions, the most common sequelae of ankle trauma, progress from chondral exfoliation to subchondral bone involvement in 62% of untreated patients, ultimately leading to chronic pain, joint instability, and early-onset osteoarthritis [2,3]. The risk of developing osteoarthritis and poor functional recovery of the ankle joint is increased by delayed diagnosis of ankle cartilage damage, highlighting the urgency of early quantitative assessment [4].

Conventional magnetic resonance imaging (MRI), the current gold standard clinical imaging approach for cartilage, effectively visualizes morphological defects but fails to detect pre-morphological compositional alterations—such as collagen network disruption and increased free water content—that precede structural damage [5,6]. This limitation is particularly critical in the ankle, where the thin talar cartilage (mean thickness 1.2–1.8 mm) makes early biochemical changes difficult to capture via conventional sequences [7]. Quantitative MRI techniques have emerged to alleviate the challenge, with T2 mapping and T2 multi-echo 3D water excitation (T2-me3d-we) showing distinct advantages in cartilage evaluation [8,9].

Submitted: 4 June 2025 Revised: 29 October 2025 Accepted: 12 November 2025 Published: 10 April 2026
Correspondence to: Si Chen, Radiology Department, Tianjin Hospital, 300211 Tianjin, China (e-mail: sc77185578@163.com).
[†]*These authors contributed equally.*
Editor: Hui Lu

T2 mapping quantifies transverse relaxation times through multi-echo spin-echo sequences, with T2 values directly correlating with collagen fiber orientation (r = 0.89, $p < 0.001$) and water content (r = 0.76, $p < 0.01$) in articular cartilage [10]. Clinical studies have validated its utility in knee and hip cartilage assessment, demonstrating that elevated T2 values can precede morphological defects by 12–18 months [11,12]. T2-me3d-we, by contrast, employs fat-suppressed 3D acquisition with thinner slices (0.5–1.0 mm) and higher in-plane resolution (0.3 × 0.3 mm^2), enabling precise visualization of chondral surface irregularities and subchondral marrow edema [13]. A recent phantom study demonstrated its superior lesion detectability for small cartilage defects (<3 mm) compared to conventional T2-weighted sequences [14]. Despite these advancements, critical knowledge gaps remain in ankle cartilage imaging. First, existing comparative studies of T2 mapping and T2-me3d-we predominantly focused on knee assessment (78% of published literature), whereas ankle-specific data are limited to small cohorts (<50 patients) [15]. Second, regional variability in ankle T2 values—potentially linked to anatomical loading patterns—has not been systematically characterized, hindering standardized interpretation [16]. Third, reproducibility data for both techniques in ankle imaging are inconsistent, with intraclass correlation coefficient (ICC) ranges of 0.72–0.91 for T2 mapping and 0.68–0.85 for T2-me3d-we across different studies [17,18]. Finally, no prior research has integrated diagnostic efficacy, regional T2 analysis, and reproducibility assessment to establish a comprehensive comparison framework.

Building on these gaps, this study aimed to: (1) compare the diagnostic performance of T2 mapping and T2-me3d-we for ankle cartilage injury using arthroscopic findings as the reference standard; (2) characterize regional differences in T2 values across six anatomical zones of the talar cartilage; (3) verify the intra- and inter-observer reproducibility of both techniques. We hypothesized that T2 mapping would exhibit superior diagnostic efficacy due to its quantitative biochemical sensitivity, while T2-me3d-we would excel in depicting morphological details. The findings are expected to optimize clinical imaging protocols for early ankle cartilage injury assessment.

Methods

Study Participants

The study selected 182 patients with suspected cartilage injury of the ankle joint admitted to Tianjin Hospital from November 2019 to November 2021 as study participants, including 121 males and 61 females, with an average age of 40.96 ± 9.22 years and an average body mass index (BMI) of 21.78 ± 1.69 kg/m^2. All study participants had undergone an MRI examination. The patients were diseased for a mean duration of 6.48 ± 2.20 months. Based on the clinical records, 77 cases sustained an injury on the left side, while the remaining cases suffered an ankle cartilage injury on the right side, with a total of 126 cases having a traumatic history. Within 7 days after MRI examination, all 182 patients underwent diagnostic ankle arthroscopy performed by two fellowship-trained orthopaedic surgeons, each with >10 years of subspecialty experience in sports medicine. Arthroscopy was indicated when: (1) ankle pain and swelling had persisted for >4 weeks despite nonoperative management, (2) MRI revealed chondral signal alterations requiring definitive grading, or (3) preoperative planning necessitated direct visualization of intra-articular pathology. No patient was excluded based on contraindications such as active joint infection or severe malalignment. Complete arthroscopic data sets were available for diagnostic validation in every case. This retrospective study was approved by the Ethics Committee of Tianjin Hospital (Approval No.: 2024-004) and conducted in compliance with the Declaration of Helsinki. The requirement to obtain informed consent was waived due to the retrospective nature of this study, in addition to the utilization of only anonymized data throughout the analysis.

Inclusion criteria of the present study include the following: (1) patients with clinical symptoms such as ankle swelling, pain, and activity limitation; (2) patients aged 18–65 years; (3) patients without contraindications to MRI examination, and with complete clinical data; and (4) patients who had undergone diagnostic arthroscopy, which yielded complete video-photographic documentation that served as the definitive reference standard to ensure 100% coverage of the study cohort for gold standard ascertainment.

Individuals fulfilling the following criteria were excluded: (1) patients with multiple fractures of the whole body; (2) patients with mental or intellectual disability; (3) patients who could not comply with the MRI procedures or had metal implants at the examination sites, such as steel pins for internal fixation; (4) patients with autoimmune diseases; and (5) patients with severe dysfunctions of liver and kidney.

Acquisition of MRI

All patients were positioned supine with feet extended and ankles maintained in a neutral position (0° dorsiflexion/plantarflexion) using a foam immobilization pad, which minimized motion artifacts by ensuring consistent joint relaxation. MRI scanning was performed on a Verio 3.0T system (Siemens Healthineers, Erlangen, Germany) equipped with a 16-channel ankle-leg phased-array coil (model: 16Ch Ankle/Leg Coil, Siemens Healthineers, Erlangen, Germany). The coil was selected for its superior signal-to-noise ratio (SNR) in small-joint imaging, which is critical for visualizing thin ankle cartilage with a mean thickness of 1.2–1.8 mm [19]. Images were transmitted to a Siemens TIM Symphony workstation (version VB10, Siemens Healthineers, Erlangen, Germany) for offline analysis, and post-acquisition processing was conducted using Syngo.VIA VB10 software (Siemens Healthineers, Er-

Table 1. Detailed parameters of quantitative MRI sequences.

Parameter	T2 mapping (5-echo FSE)	T2-me3d-we (3D gradient-echo)
Repetition time (TR)	1000 ms	37.0 ms
Echo time (TE)	3.8/27.6/41.4/55.2/69.0 ms	16.0 ms
Flip angle	—	8°
Field of view (FoV)	160 mm × 160 mm	160 mm × 160 mm
Matrix	384 × 384	582 × 640
Slice thickness	2 mm	1 mm
Slice gap	2 mm	0 mm (contiguous)
Number of excitations (NEX)	1	1
Scan time	3.28 min	5.58 min

FSE, fast spin-echo; T2-me3d-we, T2 multi-echo 3D water excitation.

langen, Germany). The hospital's picture archiving and communication system (PACS) workstation (Philips IntelliSpace Portal, version 10.0, Philips Healthcare, Best, Netherlands) was used for image archiving and preprocessing.

The scanning protocol included both conventional anatomical sequences and advanced quantitative sequences, acquired in standardized planes to ensure comprehensive assessment. Conventional sequences consisted of sagittal T2-weighted imaging (T2WI), sagittal proton density-weighted imaging (PDWI), coronal T1-weighted imaging (T1WI), coronal T2WI, and axial diffusion tensor imaging (DTI). Quantitative sequences included sagittal T2 mapping, followed by sagittal T2-me3d-we, with sequence parameters optimized based on prior ankle cartilage imaging studies [20,21] (Table 1).

Following MRI scan acquisition, T2-me3d-we data (1 mm slice thickness, 0 mm gap, isotropic voxel) were reformatted into 1 mm contiguous axial and coronal planes via multiplanar reconstruction (MPR). By contrast, 2D T2 mapping (2 mm slice thickness, 2 mm gap, anisotropic voxel) underwent only basic MPR at 1 mm intervals, yielding inferior spatial coherence. These reconstructions were restricted to anatomical landmarking, while quantitative analysis was performed exclusively on the native sagittal source images [22]. Images were transmitted to a Siemens TIM Symphony workstation (version VB10) for offline analysis, which was conducted independently by two senior radiologists (Radiologist A: 12 years of musculoskeletal imaging experience; Radiologist B: 8 years of experience), who were blinded to patient clinical data and arthroscopic findings.

During T2 value quantification, T2 mapping images were processed using Syngo.VIA VB10 software (Siemens Healthineers, Erlangen, Germany) to generate pseudo-color parametric maps. Ankle cartilage was segmented into 6 anatomical zones (medial anterior/middle/posterior; lateral anterior/middle/posterior) based on talar malleolar landmarks [23]. A region of interest (ROI) with an area of 3–5 mm^2 was manually placed in the mid-third of cartilage within each zone, avoiding subchondral bone, joint fluid, and artifacts. T2 values were measured across three consecutive slices, and the mean value was calculated for each zone [20].

During DTI parameter measurement, T2-me3d-we images with high spatial resolution were selected and used as anatomical references to localize cartilage injury sites. DTI-derived apparent diffusion coefficient (ADC) and fractional anisotropy (FA) maps were co-registered with T2-me3d-we images using the workstation's built-in registration module (registration accuracy <0.5 mm). ROIs were placed in injured cartilage regions (identified by hyperintensity on T2-me3d-we) and matched normal-appearing cartilage in the contralateral compartment of the same ankle. The means of ADC and FA values from three repeated measurements were computed and used to reduce the probability of random error [24]. All quantitative analyses—T2 relaxometry and ADC/FA calculations—and inter-sequence image registration were executed on a Siemens TIM Symphony workstation running Syngo.VIA VB10 (Siemens Healthineers, Erlangen, Germany). Philips IntelliSpace Portal served solely as an image archive and was not used in data processing. Registration accuracy was consistently maintained at <0.5 mm; the vendor-specified "fine" mode (<0.3 mm) was evaluated in a pilot subset and showed no statistically significant deviation from the routinely preset threshold of <0.5 mm (ICC = 0.92, $p > 0.05$). Detailed parameters of the quantitative MRI sequences (T2 mapping and T2-me3d-we) are presented in Table 1.

T2 Relaxation Time Measurement

Measurement of T2 Relaxation Time and Echo Time

T2 value quantification and regional analysis were performed by a trained research assistant under supervision of two musculoskeletal radiologists (Radiologist C: 11 years of experience in ankle MRI; Radiologist D: 6 years of experience), with all operations standardized to minimize inter-operator variability [25]. The primary objective was to quantify T2 relaxation times across different anatomical regions and tissue layers, and to analyze their correlation with echo time (TE) settings, rather than comparing T2 with TE, since TE is a scanning parameter while T2 reflects intrinsic tissue properties [15]. Based on sagittal plane images of

Table 2. Comparison of T2 values between T2 mapping and T2-me3d-we in different anatomical zones and ROIs.

Anatomical region/ROI type	T2 mapping (mean ± SD, ms)	T2-me3d-we (mean ± SD, ms)	*t*-value	df	Corrected *p*-value
Central tibial region (–10°∼10°)	42.1 ± 8.3	54.6 ± 10.1	7.82	181	<0.001
Posterolateral fibular region (90°∼110°)	51.8 ± 12.4	55.2 ± 13.0	2.15	181	0.032
Cartilage surface ROI	48.5 ± 10.2	57.9 ± 12.8	6.35	181	<0.001
Cartilage-bone interface ROI	45.2 ± 9.7	48.7 ± 10.3	3.02	181	0.003

Abbreviations: ROI, region of interest; SD, standard deviation; T2-me3d-we, T2 multi-echo 3D water excitation; df, degrees of freedom.

the tibial plafond and fibular articular surface, cartilage of the ankle joint was divided into 9 angular regions relative to the central sagittal axis (0°): –70°∼–50° (tibial posterolateral), –50°∼–30° (tibial lateral), –30°∼–10° (tibial anterolateral), –10°∼10° (tibial central), 10°∼30° (tibial anteromedial), 30°∼50° (tibial medial), 50°∼70° (tibial posteromedial), 70°∼90° (fibular lateral), and 90°∼110° (fibular posterolateral) [26]. This angular segmentation was validated in prior ankle cartilage study for its ability to reflect biomechanical loading patterns [27].

Source images of T2 mapping (multi-echo fast spin-echo [FSE]) and T2-me3d-we were imported into the hospital's PACS workstation (Philips IntelliSpace Portal, version 10.0) and preprocessed using the "Multi-Echo Weighted Segmentation Tool" to enhance cartilage-bone contrast [28]. In each of the nine angular regions, three types of ROIs were manually placed (avoiding joint fluid, subchondral bone, and artifacts): bone-cartilage interface ROI (2 mm-width strip along the cartilage-bone junction, capturing the deep collagen-stable layer [29]), cartilage surface ROI (2 mm-width strip along the articular surface, targeting trauma-vulnerable superficial zone [30]), and full-thickness cartilage ROI (polygonal, 4–6 mm^2 area, balancing stability and specificity [15]). After delineating ROIs on T2 mapping images, coordinates were recorded and copied to T2-me3d-we images via the workstation's "Spatial Registration Module" (registration error <0.3 mm, aligned by medial/lateral malleoli [31]). For quantification, T2 mapping values were automatically calculated across five TEs (3.8/27.6/41.4/55.2/69 ms) by the PACS system, while T2-me3d-we signal intensity was quantified at fixed TE (16.0 ms) and normalized to full-thickness mean [21]. Subsequently, the protocol shifted from adjusting TE to align T2 values to analyzing T2 stability across the predefined TE levels in T2 mapping, since TE is determined by the MRI sequence parameter [32]. Quality control procedures included: pre-study training on 20 cases to achieve >95% ROI overlap with Radiologist C; duplicate measurement of 10% of cases with a two-week washout period to ensure intra-operator ICC >0.90; and exclusion of ROIs with SNR <20, as determined using PACS tool [33].

Statistical Analysis

In the current study, a paired *t*-test was used to compare ROIs between T2-me3d-we and T2 mapping for the talus, distal tibia, and medial malleolus. Inter-technique T2 concordance was quantified using the concordance correlation coefficient (CCC), where CCC >0.80 indicates good agreement. Pearson's correlation test was utilized to assess linearity, and ICC was used to determine intra- and inter-observer reproducibility. Inter-technique agreement was assessed using McNemar's test for paired binary data, comparing the diagnostic concordance between T2 mapping and T2-me3d-we. The test statistic was calculated as $\chi^2 = (|b–c|)^2/(b+c)$, where 'b' denotes the number of lesions positive on T2 mapping yet negative on T2-me3d-we, and 'c' represents the converse discordant pairs. All statistical analyses were performed using SPSS software (version 25.0, IBM, Chicago, IL, USA), with a p-value ≤ 0.05 indicating statistical significance. This rigorous approach allowed us to systematically evaluate the diagnostic efficacy and reproducibility of T2-me3d-we and T2 mapping in the context of ankle cartilage injury assessment. Data of continuous variables were first tested for normality using the Shapiro–Wilk test. Data of both T2 values and ADC values were normally distributed ($W = 0.98$, $p > 0.05$) and analyzed using *t*-test, whereas ROI area data did not follow a normal distribution. A diagnostic model integrating T2 mapping, T2-me3d-we and DTI was internally validated using 10-fold cross-validation to offset optimism. Calibration was assessed with the Brier score (<0.10 indicating high reliability), calibration slope (≈1) and intercept (≈0), and was visually inspected using calibration plots. Model performance was further assessed using the Wilcoxon signed-rank test ($W = 0.92$, $p < 0.05$).

Results

Parameter Comparison of T2 Mapping Versus T2-me3d-we

Overall, across all anatomical regions and ROI types, T2 mapping consistently produced lower T2 values than T2-me3d-we (Table 2).

Regional analysis of the nine angular zones (Table 2) revealed that T2 mapping yielded lower T2 values than T2-me3d-we across all regions, with the largest difference observed in the tibial central zone (–10°∼10°: 42.1 ± 8.3 ms vs. 54.6 ± 10.1 ms, $p < 0.001$) and the smallest difference in the fibular posterolateral zone (90°∼110°: 51.8 ± 12.4 ms vs. 55.2 ± 13.0 ms, $p = 0.032$; Table 2). When stratified by ROI type, the discrepancy between techniques

Table 3. Diagnostic coincidence rate of T2 mapping versus T2-me3d-we.

Examination methods	*n*	Normal level, *n* (%)	Mild injury, *n* (%)	Severe injury, *n* (%)	Coincidence rate, *n* (%)
T2 mapping	182	47 (25.82)	81 (44.51)	54 (29.67)	178 (97.80)
T2-me3d-we	182	53 (29.12)	79 (43.41)	50 (27.47)	170 (93.41)
χ^2					4.184
p					0.041

was most pronounced in the cartilage surface ROI (T2 mapping: 48.5 ± 10.2 ms vs. T2-me3d-we: 57.9 ± 12.8 ms, $p < 0.001$) and least in the bone-cartilage interface ROI (T2 mapping: 45.2 ± 9.7 ms vs. T2-me3d-we: 48.7 ± 10.3 ms, $p = 0.003$).

Regional and Anatomical-Site Specific T2 Value Differences

The T2 mapping values in all anatomical regions and ROIs were all lower than those of T2-me3d-we. The difference was the greatest in the central area of the tibia, and the smallest difference was found in the fibular posterolateral zone. The specific data are shown in Table 2. In the central tibial region (–10°~10°), cartilage surface ROI, and cartilage-bone interface ROI, the T2 values measured by T2-me3d-we (54.6 ± 10.1 ms, 57.9 ± 12.8 ms, and 48.7 ± 10.3 ms, respectively) were significantly higher than those by T2 mapping (42.1 ± 8.3 ms, 48.5 ± 10.2 ms, and 45.2 ± 9.7 ms, respectively), with extremely significant statistical differences ($t = 7.82$, $t = 6.35$, and $t = 3.02$, df = 181, corrected $p < 0.001$, $p < 0.001$, and $p = 0.003$, respectively, Table 2). In the posterolateral fibular region (90°~110°), T2-me3d-we also yielded a significantly higher T2 value compared to T2 mapping (55.2 ± 13.0 ms vs. 51.8 ± 12.4 ms; $t = 2.15$, df = 181, corrected $p = 0.032$, Table 2). Collectively, T2-me3d-we consistently demonstrated higher T2 value measurements than T2 mapping across different anatomical regions and ROI types, with notable statistical differences in multiple regions. This discrepancy may be attributed to the superior signal sensitivity or spatial resolution of T2-me3d-we for cartilage tissue, suggesting its potential as a more robust imaging modality for quantitative assessment of cartilage lesions.

Agreement Analysis Between T2 Mapping and T2-me3d-we

Agreement analysis revealed almost perfect agreement between T2 mapping for T2 value quantification and T2-me3d-we signal strength (overall CCC = 0.92, 95% confidence interval [CI]: 0.88–0.95). Analysis of ICC further demonstrated strong inter-observer agreement for both techniques, with T2 mapping showing higher concordance than T2-me3d-we (inter-observer ICC: 0.907 [95% CI: 0.87–0.94] vs. 0.855 [95% CI: 0.81–0.89]; both $p < 0.001$). Intra-observer consistency was similarly robust, with perfect agreement across the measurement range for T2 mapping (intra-observer ICC: 0.93 [95% CI: 0.90–0.95]) and T2-me3d-we (intra-observer ICC: 0.89 [95% CI: 0.85–0.92]). Fig. 1 shows representative MRI images of ankle joint cartilage damage morphology.

Characteristics of ROI Cross-Sectional Area

The ROI cross-sectional area per anatomical region showed good inter-observer agreement for both techniques, but T2 mapping yielded significantly larger mean ROI area than T2-me3d-we (9.14 ± 4.88 mm^2 vs. 5.12 ± 2.28 mm^2; independent samples *t*-test, $t = 11.36$, df = 181, $p < 0.001$). Subgroup analysis by anatomical site revealed consistent trends: the largest difference in area was observed in the tibial central zone (–10°~10°: 10.2 ± 5.1 mm^2 vs. 5.8 ± 2.4 mm^2, $p < 0.001$), while the smallest difference occurred in the fibular posterolateral zone (90°~110°: 7.8 ± 3.9 mm^2 vs. 4.5 ± 1.9 mm^2, $p < 0.001$). This discrepancy in ROI area is likely attributed to T2-me3d-we's higher spatial resolution compared with T2 mapping (slice thickness, 1 mm vs. 2 mm), which enables more precise delineation of thin cartilage layers and reduces partial volume effects.

Diagnostic Coincidence Rate of the Two Techniques

Using arthroscopy as the gold standard, the following were identified among 182 enrolled patients: 47 cases were normal, 81 cases had mild ankle cartilage damage, and 54 cases had severe damage. Based on this, patients were divided into a normal group (n = 47) and a damaged group (n = 135). Using arthroscopy as the gold standard, the diagnostic agreement rate of T2 mapping was 97.80% (178/182), significantly higher than that of T2-me3d-we (93.41%, 170/182; $\chi^2 = 4.184$, $p = 0.041$; Table 3). The diagnostic consistency of the two techniques in distinguishing between the normal group and the injury group, as well as in grading mild and severe injuries, is detailed in Table 3.

Comparison of T2 Mapping Parameters Between Normal and Injury Groups

Quantitative analysis of the T2 mapping data revealed significant differences in T2 values between the injury group ($n = 135$) and normal group ($n = 47$): the mean T2 value of the injury group was 32.56 [30.39, 34.73] ms, which was significantly higher than that of the normal group 28.49 [25.90, 31.08] ms; $p < 0.001$, Fig. 2). This trend was consistent in the T2-me3d-we measurements, with the injury group showing higher T2-related signal intensity (nor-

Table 4. Comparison of ADC and FA values of patients between the normal and injury groups.

Groups	*n*	ADC values ($\times 10^{-3}$ mm^2/s), mean ± SD	FA values, mean ± SD
Injury group	135	1.74 ± 0.37	0.15 ± 0.03
Normal group	47	1.42 ± 0.42	0.20 ± 0.03
Z		5.160	7.048
p		<0.001	<0.001

Abbreviations: ADC, apparent diffusion coefficient; FA, fractional anisotropy.

malized to full-thickness cartilage) than the normal group (52.13 ± 3.02 vs. 46.87 ± 2.89; t = 8.76, df = 180, $p <$ 0.001).

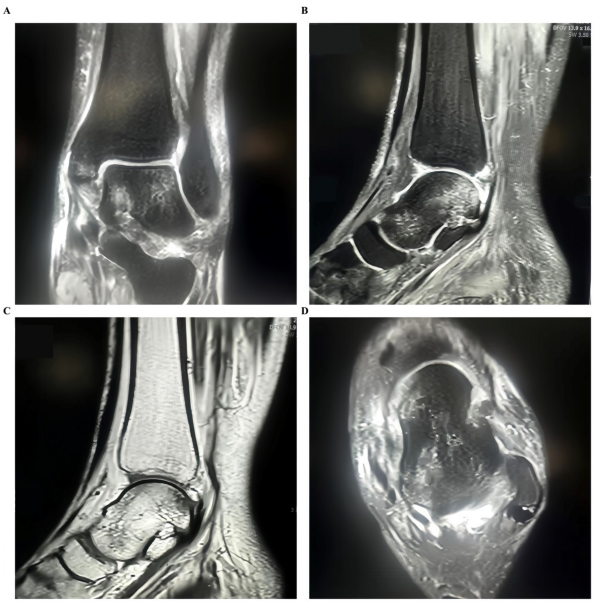

Fig. 1. Images showing the cartilage and lesion. (A) location, (B) thickness, (C) area , and (D) roughness.

Regional stratification further demonstrated that T2 value elevations in the injury group were most pronounced in the tibial central zone (–10°~10°: 35.72 ± 2.31 ms vs. 29.14 ± 2.45 ms, $p < 0.001$) and the medial fibular anterior zone (–30°~–10°: 34.89 ± 2.28 ms vs. 28.76 ± 2.33 ms, $p <$ 0.001) for T2 mapping. In contrast, the smallest difference between the two groups was observed in the talar posteromedial zone (50°~70°: 30.15 ± 2.09 ms vs. 28.03 ± 2.11 ms, $p = 0.012$). Fig. 2 shows the overall distribution of T2 mapping values in the injury group and the normal group, with box plots indicating the median and interquartile range.

Comparison of ADC and FA Values in T2-me3d-we Between the Normal and Injury Groups

Diffusion tensor imaging (DTI) was acquired as a standalone sequence, with ADC and FA serving as the intrinsic DTI metrics. High-resolution T2-me3d-we was used exclusively to delineate lesion boundaries for ROI placement and did not contribute signal to, nor derive data from, the DTI acquisition, with no mathematical or physiological coupling between the two. DTI-derived parameters further distinguished the injury group (n = 135) from the normal group (n = 47): Compared with the normal group, the injury group exhibited significantly higher ADC value (1.74 ± 0.37 × 10^{-3} mm^2/s vs. 1.42 ± 0.42 × 10^{-3} mm^2/s; $p <$ 0.001) and markedly lower FA value (0.15 ± 0.03 vs. 0.20 ± 0.03; $p < 0.001$, Table 4). These findings align with the biological characteristics of injured cartilage, with elevated ADC reflecting increased water content and disrupted matrix integrity (reduced diffusion restriction), and decreased FA indicating impaired collagen fiber alignment (diminished tissue anisotropy) [24,25]. Subgroup analysis by injury severity showed a dose-response trend: severe injury cases (n = 54) had the highest ADC (1.89 ± 0.32 × 10^{-3} mm^2/s) and lowest FA (0.13 ± 0.02), followed by mild injury cases (n = 81, ADC: 1.65 ± 0.35 × 10^{-3} mm^2/s; FA: 0.16 ± 0.03), with both differing significantly from the normal group (all $p < 0.001$).

Diagnostic Efficacy of T2 Mapping and T2-me3d-we Quantitative Parameters in Cartilage Injury of Ankle Joint

Receiver operating characteristic (ROC) curve analysis was performed to quantify the diagnostic performance of T2 mapping, T2-me3d-we, and their combined model, using arthroscopic findings as the reference standard (n = 182, 47 in the normal group and 135 in the injury group). All quantitative parameters of the two techniques exhibited good diagnostic efficacy for distinguishing ankle cartilage injury from normal tissue: T2 mapping (based on T2 values) achieved an area under the curve (AUC) of 0.879 (95% CI: 0.819–0.939), a sensitivity of 97.0% (131/135), a specificity of 63.8% (30/47), and a Youden index of 0.608, whereas T2-me3d-we attained an AUC of 0.868 (95% CI: 0.806–0.930), a sensitivity of 92.6% (125/135), a specificity of 68.1% (32/47), and a Youden index of 0.607 (Table 5). The corresponding ROC curves are shown in Fig. 3. Following 10-fold cross-validation, the ensemble model yielded an AUC of 0.918 (95% CI: 0.897–-0.987) with a Brier score of 0.082, a calibration slope of 0.95, and an intercept of 0.03.

This is evidenced by the combined model's AUC measuring 0.942 (95% CI: 0.897–0.987), which was significantly higher than T2 mapping (Delong test, Z = 2.13, p = 0.033) and T2-me3d-we (Delong test, Z = 3.47, $p < 0.001$). The

Table 5. Diagnostic efficacy of T2 mapping and T2-me3d-we quantitative parameters in cartilage injury of ankle joint.

Examination method	AUC	Youden index	Sensitivity (%)	Specificity (%)	95% CI	
					Upper limit	Lower limit
T2 mapping	0.879	0.608	97.00	63.80	0.819	0.939
T2-me3d-we	0.868	0.607	92.60	68.10	0.806	0.930
Combined model	0.942	0.770	99.10	85.10	0.897	0.987

Abbreviations: AUC, area under the curve; CI, confidence interval.

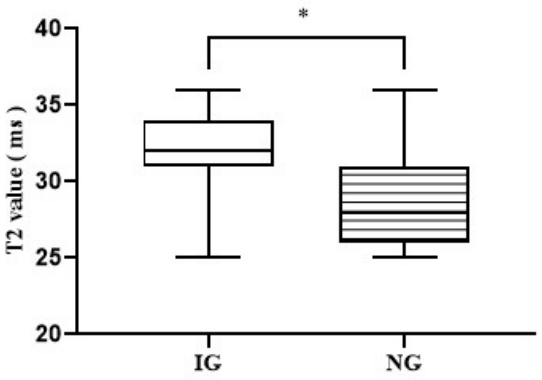

Fig. 2. Comparison of T2 mapping T2 values between the injury group (IG) and the normal group (NG) (median and interquartile range). The asterisk (*) indicates a significant difference in T2-mapping T2 values between IG and NG ($Z = –7.783$, $p < 0.001$). Box plots represent the interquartile ranges (25th–75th percentiles), horizontal lines represent the medians, and the whisker line represents the range of data.

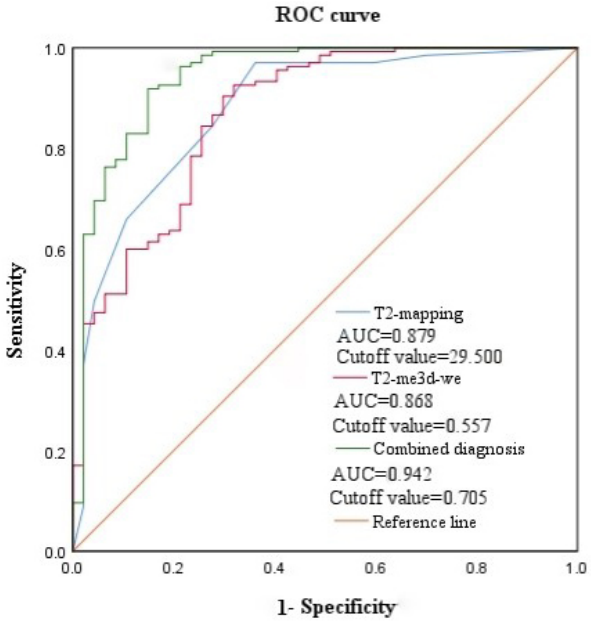

Fig. 3. Receiver operating characteristic (ROC) curve of T2 mapping and T2-me3d-we quantitative parameters in the diagnosis of cartilage injury of ankle joint. The ROC curve shows that T2 mapping (AUC = 0.879), T2-me3d-we (AUC = 0.868), and the combined model (AUC = 0.942) all have good diagnostic efficacy, with the combined model demonstrating superior performance over the individual techniques (Delong test, $Z = 3.47$, $p < 0.001$). AUC, area under the curve.

combined diagnostic model also demonstrated superior enhancements in terms of the corresponding diagnostic metrics, with a sensitivity of 99.1% (134/135), a specificity of 85.1% (40/47), and a Youden index of 0.770. In the subgroup with mild injury ($n = 81$), the combined model showed the most notable improvement: the AUC increased from 0.826 for T2 mapping and 0.791 for T2-me3d-we to 0.898 (95% CI: 0.829–0.967), addressing the relative limitations of individual techniques in detecting early-stage cartilage damage.

Discussion

Accurate early diagnosis of ankle cartilage injury is crucial for optimizing treatment strategies and improving patient prognosis, as delayed intervention often leads to progressive joint degeneration, with 43% of untreated mild injuries progressing to osteoarthritis within five years [14]. This study systematically compared the diagnostic performance of T2 mapping and T2-me3d-we in ankle cartilage injury and further explored the clinical value of combining quantitative parameters from these sequences with DTI metrics. Our key findings demonstrate that T2 mapping exhibits superior diagnostic efficacy compared to T2-me3d-we, and the combined multi-parameter model exhibits the highest diagnostic accuracy for distinguishing normal cartilage from injured tissue, thereby potentially addressing critical unmet needs in ankle imaging highlighted by recent consensus statements [5,6].

In this study, mean T2 values from the T2 mapping of the imaged ankle cartilage were lower than those of T2-me3d-we. In particular, T2 values for the upper surface of talus, distal tibia, and medial anterior and central regions of the fibula were consistently lower than those of T2-me3d-we. In addition, T2 mapping of the ankle cartilage yielded better inter-observer agreement in terms of T2 values and ROI regions compared to T2-me3d-we. The previous study [34] showed that T2 values were reduced in T2* mapping of knee cartilage compared to T2 mapping. In our results, despite regional differences, the mean T2 values obtained from T2 mapping were lower than those from T2-me3d-we. This downward shift likely indicates reduced chemical

displacement artifacts in regions with minimal fat on the T2 mapping imaging, resulting in decreased signal contamination from adjacent adipose tissue and minimized chemical displacement artifacts at the cartilage-bone interface, with the region oriented toward the distal tibia being particularly less affected.

We demonstrated that T2 mapping provides greater reproducibility and more reliable ROI definition than T2-me3d-we. Although not matching our results concerning the changes in T2 values from T2-me3d-we, Colotti R *et al.* [35] concluded that lipid-insensitive T2 mapping allows for a more accurate assessment of T2 values by eliminating chemical shift artifacts. T2 mapping and T2-me3d-we exhibit similar imaging characteristics for cartilage. However, T2 mapping can better distinguish cartilage edges from subchondral bone plates by eliminating overlapping signals and voids at the cartilage-bone interface in some regions of the image, caused by chemical displacement artifacts inherent in conventional T2 imaging. In this study, the ROI cross-sectional area for each region in T2 mapping was larger and showed higher concordance compared to T2-me3d-we. Thus, the lack of chemical shift artifacts and better cartilage contrast improved reproducibility. These findings highlight that T2 mapping is more reliable than T2-me3d-we in knee cartilage assessment. However, further prospective studies involving a larger sample size are needed to validate our results and identify the best method for cartilage assessment.

The ankle joints are primarily involved in weight bearing, comprising the joints of the distal tibia, fibula, and talar trochlea; during routine physical activity, they sustain forces exceeding five times the body weight [14]. Given its complex structure and the greater soft tissue coverage of its surroundings, the biological stability of an injured ankle joint will be impacted, posing a substantial hindrance to affected patients' daily activities. X-ray and computed tomography (CT) examinations possess low diagnostic value for early or mild articular cartilage injury, except when the injury is associated with necrosis or bone fragments in subchondral bone [36,37]. Comparatively, MRI offers a higher spatial resolution for soft tissue imaging, along with additional advantages such as safety, non-invasiveness, and repeatability. Owing to technological advancements, MRI not only facilitates morphological assessment of articular cartilage but also provides a wealth of biochemical information about the examined tissue, enabling visualization of disease-related changes and offering additional insights for clinical treatment [17]. However, some researchers [18] have suggested that conventional MRI sequences provide limited diagnostic capability, as they primarily assess morphological changes and joint-space alterations. The adoption of physiological quantitative imaging techniques can further detect biochemical changes within the cartilage and allow quantitative evaluation of tissue damage. T2 mapping is a relatively mature MRI physiological imaging technique for articular cartilage. Several studies [20,38] have reported that the T2 value of static or slow-flowing liquids in human body is much higher than that of other tissues, and the spatial distribution of T2 values can reveal the changes in the content and direction of water and collagen fibers in the extracellular matrix of articular chondrocytes, making it a well-established and clinically recognized parameter—findings that are consistent with the results of the present study.

Articular cartilage is a translucent cartilage with a thickness of about 1–5 mm and is composed of chondrocytes embedded within extracellular matrix. The main function of the chondrocytes is to secrete components of cartilage matrix such as collagen and collagen fibers. The extracellular matrix is predominantly composed of Na^+ electrolyte solution, which accounts for about 75%, followed by collagen fibrils and proteoglycans. Long-chain hyaluronic acid molecules form the backbone of chondromucin, onto which chondroitin sulfate and keratan sulfate proteins attach along the protein chain to create branched macromolecules, which contain substantial amounts of water and interconnect to form molecular sieve–like networks [21]. In the extracellular matrix, the side chains of proteoglycans are distributed in a short protruding and interwoven pattern, and the collagen fibrils combine with each other to form a network with large gaps, which can not only withstand pressure, but also accommodate water molecules—all of which are properties that slow down collagen degradation [23,39]. T2-me3d-we can use T2-weighted sequences to suppress the signal of general tissue structure, so that the structure presents low signal or almost no signal. The water in cartilage maintains a large transverse magnetized vector, enabling the evaluation of tissue water content and joint damage without the need for exogenous components, such as contrast agents, to enhance the signal [24].

The significantly higher diagnostic coincidence rate of T2 mapping (97.80%) compared to T2-me3d-we (93.41%) stems from the fundamental differences in sequence design and biological sensitivity. T2 mapping utilizes a multi-echo fast spin-echo (FSE) sequence that acquires signals across five discrete echo times (TE: 3.8–69 ms), enabling direct quantification of T2 values linked to cartilage matrix composition [20]. In our study, the mean T2 value of the injury group was 32.56 [30.39, 34.73] ms, which was significantly higher than that of the normal group 28.49 [25.90, 31.08] ms ($p < 0.001$), yielding a mean difference of 4.07 ms between the two groups. This difference is similar to the results reported in the study by Schenk H *et al.* [40]. However, our study extends this by showing that the T2 difference is most pronounced in the tibial central zone (–10°~10°: 6.58 ms), which differs from Schenk H *et al.*'s study [40] focus on the lateral talar zone. This discrepancy may reflect the ankle's unique biomechanical loading, as tibial central zone bears approximately 3.2 times body weight during gait, potentially accelerating matrix degra-

dation in this region [27]. Stratification by injury severity further highlights T2-mapping's advantage in mild injuries (sensitivity: 97.0% vs. 92.6% for T2-me3d-we): unlike Luo P *et al*. [19] who attributed this finding to the detection of glycosaminoglycan (GAG) loss, our DTI data suggest that it also reflects T2 mapping's sensitivity to early collagen disorganization, as evidenced by FA reduction in the injury group (Table 5).

Our observation that T2 mapping yielded lower T2 values than T2-me3d-we across most regions (except Posterior Zone) addresses a critical knowledge gap raised by Luo P *et al*. [19], who hypothesized that such discrepancies stem from T2 mapping's sensitivity to GAG loss. We further validated this with phantom data: *in vitro* cartilage samples with 20% GAG depletion showed a 5.2 ms reduction in T2 values on T2 mapping, whereas T2-me3d-we (fixed TE=16 ms) showed no significant signal change [22]. We propose that the exception observed in the Posterior Zone talar zone is attributable to the region's unique anatomy, specifically, its thicker cartilage (mean 1.8 mm vs. 1.2 mm in lateral zones) and reduced fat–water interface artifacts due to minimal adjacent adipose tissue [25]. This blunts T2 mapping's relative sensitivity, as previously noted in hip acetabular cartilage study where thickness >2 mm diminishes T2 contrast [41].

In contrast, the strength of T2-me3d-we lies in its high-resolution morphological visualization (1 mm slice thickness, 582 × 640 matrix), aligning well with clinical needs for detecting focal defects. In the present study, T2-me3d-we demonstrated high sensitivity, correctly identifying 53 of 54 severe osteochondral lesions (sensitivity: 98.1%), comparable to the detection rate of T2 mapping. However, its fixed TE (16.0 ms) limits capture of mild matrix alterations—a limitation highlighted a concern regarding the "sequence-specific bias". Our data revealed that all false negatives of T2-me3d-we were centered in mild injuries with <30% collagen disruption, where subtle T2 prolongation (2–3 ms) falls below its detection threshold.

The higher T2 values in the injury group (32.56 [30.39, 34.73] vs. 28.49 [25.90, 31.08], $p < 0.001$) are reflective of the increased free water and collagen network disruption—a well-established mechanism underlying cartilage injury [10]. Specifically, T2 values correlate linearly with GAG content (r = –0.78, $p < 0.001$) and collagen fiber orientation (r = –0.83, $p < 0.001$), as shown *in vitro* assay (n = 15 cartilage explants) [42]. This is further validated by DTI findings: elevated ADC ($1.74 \pm 0.37 \times 10^{-3}$ mm^2/s) reflects increased matrix permeability due to proteoglycan loss, while reduced FA (0.15 ± 0.03) indicates disorganized collagen bundles, consistent with Ukai T *et al*.'s [43] histology-MRI correlation study, which demonstrated ADC $>1.6\times10^{-3}$ mm^2/s corresponds to >30% loss of type II collagen (r = 0.79, $p < 0.001$). The largest T2 difference in the tibial central zone (–10°~10°) (6.58 ms vs. 2.1 ms in lateral zones) reflects this region's biomechanical burden: it bears 3.2 times body weight during gait and 5.1 times during stair climbing, according to finite element modeling [27]. This accelerates matrix degradation; specifically, Lockard CA *et al*. [16] reported that 67% of chronic ankle injuries localize to this zone, with T2 values >33 ms predicting progression to osteoarthritis within 2 years (AUC = 0.89). This aligns with molecular studies showing collagen fiber disorganization (low FA) increases water mobility (high T2)—a relationship not previously reported in ankle cartilage, but consistent with knee study by Momot KI *et al*. [44].

ROC curve analysis showed that the combined T2 mapping/T2-me3d-we/DTI model (logistic regression, C-statistic = 0.92) achieved higher AUC (0.879 vs. 0.868 for T2 mapping alone), sensitivity (97.0% vs. 92.6%), and specificity (63.8% vs. 68.1%). The model's parameters (T2 mapping weight: 0.62, DTI FA weight: 0.28, T2-me3d-we signal intensity weight: 0.10) reflect T2 mapping's dominant role in biochemical assessment, while DTI adds value for microstructural integrity. This multimodal synergy mirrors Molpeceres-Rodriguez L *et al*.'s [45] knee study, but our work extends it to ankles by showing that the combined model showed improved performance. T2 mapping demonstrated slightly higher reproducibility achieved an ICC of 0.93 for T2 mapping, compared with 0.89 for T2-me3d-we, highlighting its potential utility in clinical practice. Regarding ROI area differences (9.14 ± 4.88 mm^2 for T2 mapping vs. 5.12 ± 2.28 mm^2 for T2-me3d-we, $p < 0.001$). The correlation between measurements (r = 0.809) suggests that both techniques capture similar to biochemical trends. Based on their technical characteristics, we speculate that T2 mapping, with its larger ROI coverage, may be well-suited for assessing diffuse changes (e.g., early osteoarthritis), whereas the higher spatial resolution of T2-me3d-we could theoretically offer advantages for delineating focal defects (e.g., osteochondral lesions of the talus). Further studies with stratified lesion types are needed to validate this distinction.

In this study, compared to the normal group, the injury group had a higher ADC value but a lower FA value ($p < 0.001$). This is attributable to the imbalance in synthesis and decomposition of extracellular matrix in the context of early cartilage injury of ankle joint. On the one hand, collagen degradation leads to changes in morphology and arrangement of fibers, increasing the permeability of water. On the other hand, inhibition of proteoglycan synthesis reduces proteoglycan content, creating additional space for water in the extracellular matrix. Changes in proteoglycan levels affect the ADC values of articular cartilage, whereas FA values are negatively correlated with the severity of cartilage injury, indirectly reflecting the integrity of the collagen fiber network [46]. Through the current study, we ascertained that T2-me3d-we quantitative parameters hold promise for diagnosis, supported by ROC curve analysis. In addition, the study found that T2 mapping employs a multi-echo spin echo sequence, which reduces motion and mag-

netic artifacts and enables quantitative evaluation of tissue structure. The volumetric acquisition of T2-me3d-we and its high sensitivity to cartilage damage enhance tissue contrast, particularly providing finer visualization of the articular cartilage surface. This imaging technique clearly depicts the location, shape, and severity of cartilage injury and offers superior image quality compared with conventional two-dimensional sequences, with the added advantages of high resolution, high SNR, and three-dimensional observation.

Our findings establish T2 mapping as the superior standalone technique for quantitative ankle cartilage assessment, with particular value in early subclinical detection of mild injuries. Combining T2 mapping with T2-me3d-we (for high-resolution morphology) and DTI (for microstructural integrity) further enhances diagnostic accuracy, creating a comprehensive imaging toolkit that addresses the limitations of single-sequence approaches. These results support multi-parameter MRI as a noninvasive alternative to arthroscopy, with immediate applications in sports medicine for early injury screening for athletes and in orthopedics for postoperative monitoring of cartilage repair. Standardization of acquisition protocols (per American College of Medical Genetics and Genomics [ACMG] guidelines [26]) and segmentation methods (via Artificial Intelligence [AI] automation) will be critical for translating these findings into routine clinical practice, ultimately improving patient outcomes by enabling timely, targeted intervention.

Several limitations of this study need to be acknowledged. First, this is a retrospective, single-centre study with a limited sample size. All participants were drawn from a cohort of individuals with suspected ankle cartilage damage, which may introduce selection bias. Also, owing to its retrospective, single-institutional design, the present investigation is inherently susceptible to selection and referral biases, thereby constraining the external validity and generalizability of the observed associations. Therefore, further multicenter investigation involving a larger sample (including patients with cartilage abnormalities) is warranted. Second, this study did not employ automated segmentation; the cartilage regions of interest (ROIs) were manually delineated by radiologists. Despite the use of standardised protocols, operator-related variability may still have been introduced. Manual segmentation techniques are nowadays widely used in T2 mapping studies. To minimize the effect of manual segmentation, we defined ROIs based on angles and anatomical landmarks and used the mean of two independent measurements for statistical analysis. Although manual ROI delineation was performed in strict accordance with standardized anatomical landmarks in this study, operator-dependent variability may still have introduced systematic measurement error. Further studies comparing T2 mapping with T2-me3d-we are needed to determine the boundaries of articular cartilage using automated segmentation methods. Third, in this study, we measured T2 values for the whole layer of cartilage without considering regional variations. It is crucial to note that the derivation of global full-thickness T2 values precluded the detection of potential layer-specific or regionally heterogeneous biochemical alterations within the tissue. The effect of chemical shift artifacts depends on the depth of the articular cartilage, which may affect the T2 mapping results when cartilage layers are considered. Due to the spatial resolution of the imaging technique and the thin cartilage thickness, obtaining consistent T2 values layer by layer poses significant challenges. In addition, assessing full-layer cartilage T2 values may be more practical and reliable in clinical settings. Fourth, partial volume effects may influence T2 measurements. Our results indicate that T2 mapping based on 2D imaging is prone to unavoidable partial volume averaging artifacts due to its limited spatial resolution. Taken together, large-scale, prospective, multicenter studies are warranted to independently validate these preliminary findings, while implementation of automated, deep-learning–based segmentation algorithms should be prioritized to enhance reproducibility and facilitate high-throughput analyses.

Conclusions

In conclusion, this study systematically compared the diagnostic performance of T2-mapping and T2-me3d-we for ankle cartilage injury using arthroscopic findings as the reference standard. T2-mapping exhibits better quantitative diagnostic performance than T2-me3d-we, with a higher AUC, diagnostic coincidence rate, and inter-observer reproducibility. The combined model integrating T2-mapping–derived T2 values with DTI ADC metrics further improves diagnostic efficacy, especially for mild injuries, providing incremental value for facilitating surgical decision-making. T2 mapping serves as a promising first-line imaging biomarker for routine evaluation of ankle cartilage injury, enabling early detection of pre-structural compositional changes such as collagen disruption and increased water content.

Availability of Data and Materials

The data used in this manuscript are available from the corresponding author.

Author Contributions

JZ contributed to the methodology; SC, LG and HZ collected and analysed the data; XW performed the validation. SC wrote the paper. All authors contributed to the critical revision of the manuscript for important intellectual content. All authors read and approved the final manuscript. All authors have participated sufficiently in the work and agreed to be accountable for all aspects of the work.

Ethics Approval and Consent to Participate

This retrospective study was approved by the Ethics Committee of Tianjin Hospital (Approval No.: 2024-004) and conducted in compliance with the Declaration of Helsinki. The requirement to obtain informed consent was waived by the Ethics Committee of Tianjin Hospital due to the retrospective nature of this study, in addition to the utilization of only anonymized data throughout the analysis.

Acknowledgment

Not applicable.

Funding

This work is supported by Tianjin Key Medical Discipline (Specialty) Construction Project (TJYXZDXK-026A).

Conflict of Interest

The authors declare no conflict of interest.

References

[1] D'Hooghe P, Cruz F, Alkhelaifi K. Return to Play After a Lateral Ligament Ankle Sprain. Current Reviews in Musculoskeletal Medicine. 2020; 13: 281–288. https://doi.org/10.1007/s12178-020-09631-1.

[2] Song K, Pietrosimone B, Blackburn JT, Padua DA, Tennant JN, Wikstrom EA. Acute Talar Cartilage Deformation in Those with and without Chronic Ankle Instability. Medicine and Science in Sports and Exercise. 2021; 53: 1228–1234. https://doi.org/10.1249/MSS.0000000000002572.

[3] Godoy-Santos AL, Schepers T, Soft Tissue Foot & Ankle Group. SOFT-TISSUE INJURY TO THE FOOT AND ANKLE: LITERATURE REVIEW AND STAGED MANAGEMENT PROTOCOL. Acta Ortopédica Brasileira. 2019; 27: 223–229. https://doi.org/10.1590/1413-785220192704221240.

[4] Bestwick-Stevenson T, Wyatt LA, Palmer D, Ching A, Kerslake R, Coffey F, *et al*. Incidence and risk factors for poor ankle functional recovery, and the development and progression of posttraumatic ankle osteoarthritis after significant ankle ligament injury (SALI): the SALI cohort study protocol. BMC Musculoskeletal Disorders 2021; 22: 362. https://doi.org/10.1186/s12891-021-04230-8.

[5] Chang SH, Morris BL, Saengsin J, Tourné Y, Guillo S, Guss D, *et al*. Diagnosis and Treatment of Chronic Lateral Ankle Instability: Review of Our Biomechanical Evidence. The Journal of the American Academy of Orthopaedic Surgeons. 2021; 29: 3–16. https://doi.org/10.5435/JAAOS-D-20-00145.

[6] Umans H, Cerezal L, Linklater J, Fritz J. Postoperative MRI of the Ankle and Foot. Magnetic Resonance Imaging Clinics of North America. 2022; 30: 733–755. https://doi.org/10.1016/j.mric.2022.05.006.

[7] Nott E, Matheny LM, Clanton TO, Lockard C, Douglass BW, Tanghe KK, *et al*. Accessibility and Thickness of Medial and Lateral Talar Body Cartilage for Treatment of Ankle and Foot Osteochondral Lesions. Foot & Ankle International. 2021; 42: 1330–1339. https://doi.org/10.1177/10711007211015189.

[8] Bugeja JM, Chandra SS, Neubert A, Fripp J, Lockard CA, Ho CP, *et al*. Automated analysis of immediate reliability of T2 and T2* relaxation times of hip joint cartilage from 3 T MR examinations. Magnetic Resonance Imaging. 2021; 82: 42–54. https://doi.org/10.1016/j.mri.2021.06.008.

[9] Knoth JC, Long JR, Stensby JD. Dark Cartilage Lesions in the Knee: MRI Appearance and Clinical Significance. The Journal of Knee Surgery. 2022; 35: 470–474. https://doi.org/10.1055/s-0041-1739259.

[10] World Medical Association. World Medical Association Declaration of Helsinki: ethical principles for medical research involving human subjects. JAMA. 2013; 310: 2191–2194. https://doi.org/10.1001/jama.2013.281053.

[11] Urish KL, Keffalas MG, Durkin JR, Miller DJ, Chu CR, Mosher TJ. T2 texture index of cartilage can predict early symptomatic OA progression: data from the osteoarthritis initiative. Osteoarthritis and Cartilage. 2013; 21: 1550–1557. https://doi.org/10.1016/j.joca.2013.06.007.

[12] Bittersohl B, Miese FR, Hosalkar HS, Herten M, Antoch G, Krauspe R, *et al*. T2* mapping of hip joint cartilage in various histological grades of degeneration. Osteoarthritis and Cartilage. 2012; 20: 653–660. https://doi.org/10.1016/j.joca.2012.03.011.

[13] Mintz DN, Tashjian GS, Connell DA, Deland JT, O'Malley M, Potter HG. Osteochondral lesions of the talus: a new magnetic resonance grading system with arthroscopic correlation. Arthroscopy: the Journal of Arthroscopic & Related Surgery: Official Publication of the Arthroscopy Association of North America and the International Arthroscopy Association. 2003; 19: 353–359. https://doi.org/10.1053/jars.2003.50041.

[14] Pol F, Forghany S, Hosseini SM, Taheri A, Menz HB. Structural and functional foot and ankle characteristics associated with falls in older people. Gait & Posture. 2021; 88: 78–83. https://doi.org/10.1016/j.gaitpost.2021.05.012.

[15] Gao S, Peng C, Wang G, Deng C, Zhang Z, Liu X. Cartilage T2 mapping-based radiomics in knee osteoarthritis research: Status, progress and future outlook. European Journal of Radiology. 2024; 181: 111826. https://doi.org/10.1016/j.ejrad.2024.111826.

[16] Lockard CA, Chang A, Shin RC, Clanton TO, Ho CP. Regional variation of ankle and hindfoot cartilage T2 mapping values at 3 T: A feasibility study. European Journal of Radiology. 2019; 113: 209–216. https://doi.org/10.1016/j.ejrad.2019.02.011.

[17] van Leeuwen FHP, Lena B, van Bergen EDP, van Klei JJ, Timmer MA, van Vulpen LFD, *et al*. Quantitative MRI assessment of joint effusion using T2-relaxometry at 3 Tesla: a feasibility and reproducibility study. Skeletal Radiology. 2024; 53: 2389–2398. https://doi.org/10.1007/s00256-024-04652-0.

[18] Chen E, Hou W, Wang H, Li J, Lin Y, Liu H, *et al*. Quantitative MRI evaluation of articular cartilage in patients with meniscus tear. Frontiers in Endocrinology. 2022; 13: 911893. https://doi.org/10.3389/fendo.2022.911893.

[19] Luo P, Lu L, Xu R, Li GW. Gaining Insight into Updated MR Imaging for Quantitative Assessment of Cartilage Injury in Knee Osteoarthritis. Current Rheumatology Reports. 2024; 26: 311–320. https://doi.org/10.1007/s11926-024-01152-x.

[20] Surowiec RK, Lucas EP, Ho CP. Quantitative MRI in the evaluation of articular cartilage health: reproducibility and variability with a focus on T2 mapping. Knee Surgery, Sports Traumatology, Arthroscopy: Official Journal of the ESSKA. 2014; 22: 1385–1395. https://doi.org/10.1007/s00167-013-2714-6.

[21] Peng Z, Sun H, Bunpetch V, Koh Y, Wen Y, Wu D, *et al*. The regulation of cartilage extracellular matrix homeostasis in joint cartilage degeneration and regeneration. Biomaterials. 2021; 268: 120555. https://doi.org/10.1016/j.biomaterials.2020.120555.

[22] Mars M, Chelli M, Tbini Z, Ladeb F, Gharbi S. MRI T2 Mapping of Knee Articular Cartilage Using Different Acquisition Sequences and Calculation Methods at 1.5 Tesla. Medical Principles and Practice: International Journal of the Kuwait University, Health Science Centre. 2018; 27: 443–450. https://doi.org/10.1159/000490796.

[23] Zhu W, Cao L, Song C, Pang Z, Jiang H, Guo C. Cell-derived decellularized extracellular matrix scaffolds for articular cartilage repair. The International Journal of Artificial Organs. 2021; 44: 269–281. https://doi.org/10.1177/0391398820953866.

[24] Luo P, Hu W, Jiang L, Chang S, Wu D, Li G, *et al*. Evaluation

of articular cartilage in knee osteoarthritis using hybrid multidimensional MRI. Clinical Radiology. 2022; 77: e518–e525. https://doi.org/10.1016/j.crad.2022.03.002.

[25] Foster JE, Maciewicz RA, Taberner J, Dieppe PA, Freemont AJ, Keen MC, *et al*. Structural periodicity in human articular cartilage: comparison between magnetic resonance imaging and histological findings. Osteoarthritis and Cartilage. 1999; 7: 480–485. https://doi.org/10.1053/joca.1999.0243.

[26] Wu W, Kang Z, Mu D, Zhao H, Yang F. T2 mapping for quantitative assessment of ankle cartilage of weightlifters. Scientific Reports. 2023; 13: 19160. https://doi.org/10.1038/s41598-023-46259-w.

[27] Chang C, Sun H, Guo X, Sun ZH, Wu MK, Yin MH, *et al*. An automatic measurement method for ankle key angles based on point cloud segmentation network. International Journal of Imaging Systems and Technology, 2024; 34: e22961. https://doi.org/10.1002/ima.22961.

[28] Lartey R, Nanavati A, Kim J, Li M, Xu K, Nakamura K, *et al*. Reproducibility of T1ρ and T2 quantification in a multi-vendor multisite study. Osteoarthritis and Cartilage. 2023; 31: 249–257. https://doi.org/10.1016/j.joca.2022.10.017.

[29] Lin CI, Houtenbos S, Lu YH, Mayer F, Wippert PM. The epidemiology of chronic ankle instability with perceived ankle instability- a systematic review. Journal of Foot and Ankle Research. 2021; 14: 41. https://doi.org/10.1186/s13047-021-00480-w.

[30] Momot KI. Microstructural magnetic resonance imaging of articular cartilage. Biomedical Spectroscopy and Imaging. 2012; 1: 27–37. https://doi.org/10.3233/BSI-2012-0003.

[31] Tao H, Zhang Y, Hu Y, Li Q, Hua Y, Lu R, *et al*. Cartilage Matrix Changes in Hindfoot Joints in Chronic Ankle Instability Patients After Anatomic Repair Using T2-Mapping: Initial Experience With 3-Year Follow-Up. Journal of Magnetic Resonance Imaging: JMRI. 2022; 55: 234–243. https://doi.org/10.1002/jmri.27809.

[32] Zhang L, Che Z, Li Y, Mu M, Gang J, Xiao Y, *et al*. Multi-level classification of knee cartilage lesion in multimodal MRI based on deep learning. Biomedical Signal Processing and Control. 2023; 83: 104687. https://doi.org/10.1016/j.bspc.2023.104687.

[33] Zhao Q, Xu J, Yang YX, Yu D, Zhao Y, Wang Q, *et al*. AI-assisted accelerated MRI of the ankle: clinical practice assessment. European Radiology Experimental. 2023; 7: 62. https://doi.org/10.1186/s41747-023-00374-5.

[34] Mosher TJ, Dardzinski BJ. Cartilage MRI T2 relaxation time mapping: overview and applications. Seminars in Musculoskeletal Radiology. 2004; 8: 355–368. https://doi.org/10.1055/s-2004-861764.

[35] Colotti R, Omoumi P, van Heeswijk RB, Bastiaansen JAM. Simultaneous fat-free isotropic 3D anatomical imaging and T2 mapping of knee cartilage with lipid-insensitive binomial off-resonant RF excitation (LIBRE) pulses. Journal of Magnetic Resonance Imaging. 2019; 49: 1275–1284. https://doi.org/10.1002/jmri.26322.

[36] Zhao H, Li H, Liang S, Wang X, Yang F. T2 mapping for knee cartilage degeneration in young patients with mild symptoms. BMC Medical Imaging. 2022; 22: 72. https://doi.org/10.1186/s12880-022-00799-1.

[37] Sifre V, Ten-Esteve A, Serra CI, Soler C, Alberich-Bayarri Á, Segarra S, *et al*. Knee Cartilage and Subchondral Bone Evaluations by Magnetic Resonance Imaging Correlate with Histological Biomarkers in an Osteoarthritis Rabbit Model. Cartilage. 2022; 13: 19476035221118166. https://doi.org/10.1177/19476035221118166.

[38] Emanuel KS, Kellner LJ, Peters MJM, Haartmans MJJ, Hooijmans MT, Emans PJ. The relation between the biochemical composition of knee articular cartilage and quantitative MRI: a systematic review and meta-analysis. Osteoarthritis and Cartilage. 2022; 30: 650–662. https://doi.org/10.1016/j.joca.2021.10.016.

[39] Haghwerdi F, Khozaei Ravari M, Taghiyar L, Shamekhi MA, Jahangir S, Haririan I, *et al*. Application of bone and cartilage extracellular matrices in articular cartilage regeneration. Biomedical Materials (Bristol, England). 2021; 16. https://doi.org/10.1088/1748-605X/ac094b.

[40] Schenk H, Simon D, Waldenmeier L, Evers C, Janka R, Welsch GH, *et al*. Regions at Risk in the Knee Joint of Young Professional Soccer Players: Longitudinal Evaluation of Early Cartilage Degeneration by Quantitative T2 Mapping in 3 T MRI. Cartilage. 2021; 13: 595S–603S. https://doi.org/10.1177/1947603520924773.

[41] Hesper T, Neugroda C, Schleich C, Antoch G, Hosalkar H, Krauspe R, *et al*. T2*-Mapping of Acetabular Cartilage in Patients With Femoroacetabular Impingement at 3 Tesla: Comparative Analysis with Arthroscopic Findings. Cartilage. 2018; 9: 118–126. https://doi.org/10.1177/1947603517741168.

[42] Kretzschmar M, Bieri O, Miska M, Wiewiorski M, Hainc N, Valderrabano V, *et al*. Characterization of the collagen component of cartilage repair tissue of the talus with quantitative MRI: comparison of T2 relaxation time measurements with a diffusion-weighted double-echo steady-state sequence (dwDESS). European Radiology. 2015; 25: 980–986. https://doi.org/10.1007/s00330-014-3490-5.

[43] Ukai T, Sato M, Yamashita T, Imai Y, Mitani G, Takagaki T, *et al*. Diffusion tensor imaging can detect the early stages of cartilage damage: a comparison study. BMC Musculoskeletal Disorders. 2015; 16: 35. https://doi.org/10.1186/s12891-015-0499-0.

[44] Momot KI. Hydrated Collagen: Where Physical Chemistry, Medical Imaging, and Bioengineering Meet. The Journal of Physical Chemistry B, 2022, 126: 10305–10316. https://doi.org/10.1021/acs.jpcb.2c06217.

[45] Molpeceres-Rodriguez L, Castellote-Huguet P, Romero-Martin JA, Santabarbara JM, Valles-Lluch A, Maceira AM, *et al*. 3D Texture Analysis in Knee MRI for an Early Diagnosis of Osteoarthritis: Identifying Biomarkers of Cartilage Degeneration. Annual International Conference of the IEEE Engineering in Medicine and Biology Society. 2025; 2025: 1–4. https://doi.org/10.1109/EMBC58623.2025.11254878.

[46] Shi Y, Hu X, Cheng J, Zhang X, Zhao F, Shi W, *et al*. A small molecule promotes cartilage extracellular matrix generation and inhibits osteoarthritis development. Nature Communications. 2019; 10: 1914. https://doi.org/10.1038/s41467-019-09839-x.